Journal of the Serbian Chemical Society
JSCS-info@shd.org.rs • www.shd.org.rs/JSCS

ACCEPTED MANUSCRIPT

Please cite this article as G. Chunag, U. Byambasuren, S. Altantsetseg, G. Yunden, S. Sukhbaatar, and D. Altansukh, *J. Serb. Chem. Soc.* (2025) https://doi.org/10.2298/JSC250422044C

Journal of the Serbian Chemical Society
JSCS-info@shd.org.rs • www.shd.org.rs/JSCS
J. Serb. Chem. Soc. **00(0)** 1-14 (2025)
JSCS–13346
Original scientific paper
Published DD MM, 2025

Pressure oxidative leaching of copper concentrate

GUNCHIN CHUNAG[1], ULZIIDELGER BYAMBASUREN[1], SARNAI ALTANTSETSEG[1], GANCHIMEG YUNDEN[1], SUKHBAT SUKHBAATAR[2] AND DORJGOTOV ALTANSUKH[1]*

[1]*Department of Chemical Engineering, School of Applied Sciences, Mongolian University of Science and Technology, Ulaanbaatar 14191, Mongolia, and* [2]*Industrial Policy Department, Ministry of Industry and Mineral Resources, Ulaanbaatar, Mongolia.*

(Received 22 April; revised 17 May; accepted 17 June 2025)

Abstract: This study investigated the oxidative leaching of copper concentrate using a mixture of ferric ions and sulfuric acid solutions. We examined the effects of various parameters, including temperature, initial sulfuric acid concentration, and slurry filtration conditions. At lower temperatures (150 °C), the leaching process resulted in the elemental sulfur and jarosite minerals formed in the solid residue. In contrast, at higher temperatures (190 °C), the solid residue contained jarosite and hematite, the most elemental sulfur-oxidizing to sulfuric acid. Under optimal conditions, a leaching temperature of 190 °C, a concentrate-to-leaching solvent (Fe^{3+} 5 g l^{-1} and H_2SO_4 50 g l^{-1}) ratio of 1:8, an oxygen pressure of 1.0 MPa, and a solid phase particle size of less than 20 µm the dissolution rate of copper reached 98% after three hours. When the sulfuric acid concentration was increased from 30 g l^{-1} to 100 g l^{-1}, the amount of copper was increased from 40 g l^{-1} to 48 g l^{-1}. Furthermore, rapid filtering of the leaching solution without cooling helped retain most of the iron in the solid phase, resulting in a relatively pure solution. The solid residue was analyzed using X-ray diffraction (XRD) and scanning electron microscopy (SEM).

Keywords: hydrometallurgy; ferric ion; chalcopyrite acidic leaching.

INTRODUCTION

The largest copper production plants are the Erdenet and Oyu Tolgoi in Mongolia. Copper products exported between 2018 and 2023, including copper concentrate, is 8.49 million tons, and cathode copper is 66.92 thousand tons.[1] Currently, cathode copper production is less than 1% of total exports, which means the basic research and production of deep processing and purification technologies for copper concentrate have taken the attention of researchers in Mongolia.

---

* Corresponding author. E-mail: gotov@must.edu.mn

https://doi.org/10.2298/JSC250422044C

Chalcopyrite is one of the most abundant minerals, accounting for about 70% of the world's copper reserves.[2–4] Galena, sphalerite, pyrite, arsine, antimony bismuth, silver, and gold also occurred as associated with the minerals.[4–6] Hydrometallurgical processing is a more efficient and environmentally friendly technology for sulfide sulfur-containing concentrates than the pyrometallurgical method.[7] Research has been increasingly conducted to separate the base metals copper and zinc from the residual solids during the autoclave dissolution of metal-containing sulfide concentrates, thereby transferring them to solution and separating silver and gold as products.[4]

Sulfuric acid is a reagent that does not decompose under the influence of temperature, has a high boiling point, is non-volatile, is reasonably cheap, does not interfere with subsequent production processes, and is recycled in the leaching process. The mineral chalcopyrite forms the majority of copper concentrates, with a high melting point and low solubility. The dissolution rate could be decreased due to the layer of elemental sulfur coat the surface of the mineral during the leaching. Hydrometallurgical processing of sulfide-containing copper concentrates is developing in atmospheric and pressure leaching (autoclave leaching).[8,9] Depending on the temperature, autoclave leaching is classified as low-temperature (<120 °C), medium-temperature (120–180 °C), and high-temperature (>180 °C).[10] Sabina Matuska et al. reported that the copper dissolution rate increased from 85% to 98% when the oxygen pressure increased from 0.5 to 2 MPa at 140 C within 3 hours in 1 M sulfuric acidic solution.[11]

The iron-containing minerals in copper concentrate are chalcopyrite and pyrite. When these minerals are treated with a sulfuric acid solution at 180–200 °C, Fe^{3+} ions are formed by the dissolution of chalcopyrite and Fe^{2+} ions by the dissolution of pyrite. At the same time, the sulfide sulfur is converted to the sulfate sulfur to form free sulfuric acid, and ferric ion hydrolysis reactions occur, as shown in the following equations (forming jarosite and hematite) .[6]

$$2FeS_2 + 7O_2 + 2H_2O = 2FeSO_4 + 2H_2SO_4 \tag{1}$$

$$4CuFeS_2 + 17O_2 + 12H_2SO_4 = 4CuSO_4 + 10H_2SO_4 + 2Fe_2(SO_4)_3 + 2H_2O \tag{2}$$

$$2FeSO_4 + H_2SO_4 + \tfrac{1}{2}O_2 = Fe_2(SO4)_3 + H_2O \tag{3}$$

The reaction for the formation of the jarosite mineral:

$$3Fe_2(SO_4)_3 + M_2SO_4 + 12H_2O = 2MFe_3(SO_4)_2(OH)_6 + 6H_2SO_4 \tag{4}$$

$$(M = Ag^+, NH_4^+, K^+, \tfrac{1}{2}\,Pb^{2+})$$

The reaction for the formation of hematite mineral:

$$2Fe_2(SO_4)_3 + 3H_2O = Fe_2O_3 + 3H_2SO_4 \tag{5}$$

$$2FeSO_4 + \tfrac{1}{2}O_2 + 2H_2O = Fe_2O_3 + 2H_2SO_4 \tag{6}$$

There are results reported as mentioned above according to technology on pressure leaching of sulfide concentrate for recovery metals.[9,12] However, a lack of research results regarding hot filtration, that is, rapid separation of the solid-liquid phase, is an effective factor in controlling the ferric ion content in the leaching solution, which is transferred directly to the electrowinning process. Ferric ions act to increase the consumption of electrical energy during electrowinning. The rapidly separating a solution from a solid phase, i.e., during the hot filtration process, ferric ions at high temperatures can undergo hydrolysis according to the following equation and precipitate out of the solution in the form of hematite.

$$Fe^{3+} + 1.5H_2O = 0.5Fe_2O_3 \quad (7)$$

However, when the solution is cooled, the reaction reverses, causing the iron to dissolve, and the solution becomes contaminated with ferric ions. Therefore, when the solution is filtered rapidly without cooling, most of the iron remains in the solid phase, and the solution has a relatively high purity.[13,14]

In this work, copper concentrate from the "Erdenet" mining plant in Mongolia was used in pressure oxidative leaching at a temperature range of 150 °C and 190 °C. We focused on comparing the leaching efficiency of iron and copper at various parameters, including temperature, initial sulfuric acid concentration, and slurry filtration conditions.

EXPERIMENTAL

Sample preparation

Copper concentrate from the "Erdenet" mining plant in Mongolia was milled in a ring mill for 5 minutes. Due to the small size of the concentrate, a wet sieving method was employed after milling, as it is challenging to dry sieve material of this fineness. The milled concentrate was sieved through a 25 μm sieve. After sieving, the concentrate was dried at 60 °C before being analyzed and used for further experiments.

Reagents

The leaching solutions were prepared by dissolving analytical grade $Fe_2(SO_4)_3$, $CuSO_4$, and H_2SO_4 (Xilong Scientific Co. Ltd in China) in deionized water. For the study on the effect of temperature, the initial concentrations of H_2SO_4 and Fe^{3+} ion were chosen as 50 g l^{-1} and 5 g l^{-1}, respectively, within a temperature range of 150 – 190 °C. To investigate the effect of sulfuric acid concentration, the initial concentrations of H_2SO_4, Fe^{3+}, and Cu^{2+} were chosen as 50 g l^{-1}, 5 g l^{-1}, and 30 g l^{-1}, respectively, with sulfuric acid concentrations ranging from 30 g l^{-1} to 100 g l^{-1}.

Apparatus and procedure

The pressure oxidation dissolution experiments were conducted using a Hastelloy autoclave (model BFK-1/8, manufactured by Welhal Borui Chemical Machinery Co., Ltd, China) equipped with a Teflon vessel. This autoclave features a PID controller, which ensures accurate temperature control within ±1 C. Throughout the experiments, both the oxygen pressure and temperature were carefully monitored. In each experiment, 240 ml of leaching solvent was added to 30 g of milled copper concentrate sample with a particle size of 25 microns. The leaching process was performed at 150 °C, 170 °C, and 190 °C under an oxygen pressure of 1 MPa. The slurry was agitated with an anchor impeller at 150 rpm for three hours to enhance oxygen saturation in the leaching solution. After completing the dissolution process, the heating was turned off, and the autoclave was allowed to cool to 80 °C. Subsequently, the resulting slurry was filtered to separate the solid residue from the pregnant leach solution. The solid and liquid phases were then analyzed using scanning electron microscopy (SEM) (TM-1000, Hitachi Inc., Japan), X-ray diffraction (XRD) (Diffractis 583 X-ray generator, Enraf-Nonius, Netherlands), and inductively coupled plasma optical emission spectrometry (ICP-OES) (PerkinElmer NexION 300Q ICP-MS, USA) for mineralogical and chemical analysis. The following equation was used to determine the metal leaching rate:

$$\varepsilon_{Me} = \frac{m_R \cdot C_R}{m_F \cdot C_F} \cdot 100\% \tag{8}$$

Where; m_R is a mass of solid residue after leaching, g; C_R is a content of metal in solid residue, %; m_F is a mass of metal concentrate, g; C_F is a content of metal in concentrate, %.

RESULTS AND DISCUSSION

Raw material analysis

The compositional characteristics of the copper concentrate were analyzed using SEM/EDS, XRD, and ICP-OES equipment. The results from the SEM/EDS analysis (Figure 1) indicate that the concentrate has a relatively large particle size of approximately 200 micrometers. It suggests that milling is necessary for effective process autoclave leaching. The content of the main elements and minerals in the concentrate was determined through ICP-OES and XRD analyses, the results presented in Tables 1 and 2.

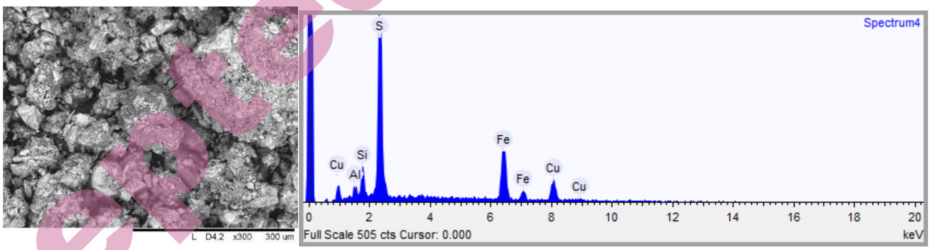

Fig 1. SEM image and EDS spectra of the copper concentrate

TABLE 1. The content of the main elements

Sample	Elements / wt/%				
	Al	Si	S	Fe	Cu
Copper concentrate	1.46	3.6	30.05	25.8	22.65

The analysis of the X-ray spectrum reveals that the concentrate is primarily composed of three elements: copper (Cu) at 22.65 %, iron (Fe) at 25.8 %, and sulfur (S) at 30.5 %. Furthermore, the X-ray diffraction analysis identifies the main minerals shown as as chalcopyrite ($CuFeS_2$) at 47.83 % and pyrite (FeS_2) at 23.79 %. The remaining minerals consist of barren rock.[15]

TABLE 2. The content of the minerals

Sample	Minerals / wt/%			
	$CuFeS_2$	FeS_2	SiO_2	$CaAlSi_2O_8$
Copper concentrate	47.83	23.79	17.13	11.24

Effect of temperature

The pressure oxidation dissolution experiments were conducted at 150 °C, 170 °C, and 190 °C, respectively, with an oxygen pressure of 1 MPa for 3 hours. The results, shown in Figure 2, indicate that as the temperature increased from 150 °C to 190 °C, the leaching rate of copper and concentration of free sulfuric acid increased when the leaching rate of iron decreased.

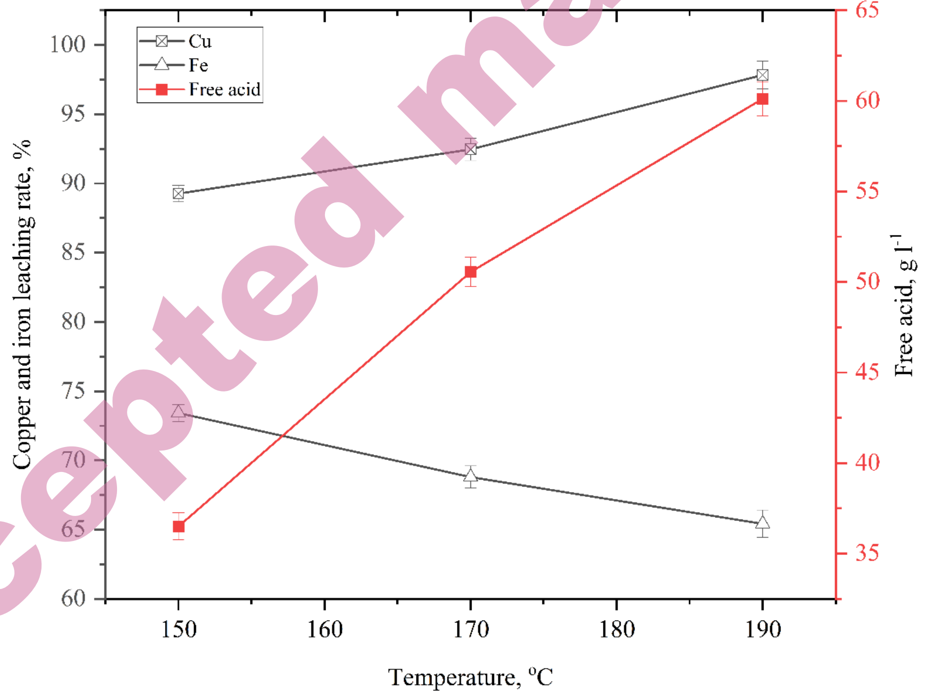

Fig 2. The effect of temperature on copper and iron leaching (initial concentration sulfuric acid 50 g l^{-1})

The pregnant leach solution and solid residue from the slurry were analyzed using ICP-OES and XRD. The results are presented in Tables 3 and 4.

TABLE 3. The composition of both the pregnant leach solution and solid residue

Temperature / °C	The composition of the pregnant leach solution / g l^{-1}			pH of the pregnant leach solution	The composition of the solid residue / wt/%		
	Cu^{2+}	Fe^{3+}	SO_4^{2-}		Cu	Fe	S (total)
150	19.0	31.5	123.9	0.87	4.5	16.8	39.09
170	21.2	30.5	144	0.56	3.73	18.3	30.32
190	22.5	26.7	147	0.56	1.34	24.5	24.3

Table 4 presents the results of the XRD analysis of the solid residue, indicating that the mass of the undissolved solid portion contains minerals such as quartz, albite, anorthite, chalcopyrite, pyrite, and various other sulfide minerals. A comparison of the mineral composition between the concentrate and the solid residue after dissolution shows that elemental sulfur may be formed during the dissolution process. The elemental sulfur of the total sulfur in the solid residue after dissolution decreased when the dissolution temperature increased.

The SEM image illustrates that small pellets or granular particles of elemental sulfur are predominant at low temperatures (see Figure 3).

TABLE 4. Mineral composition of solid residue after the leaching

Temperature / °C	Minerals, wt/%					
	$Na(AlSi_3O_8)$	S	FeS_2	SiO_2	$CuFeS_2$	$[H_3O]Fe_3[SO_4](OH)_6$
150	28.45	23.26	16.36	13.64	10.75	7.69
170	22.70	18.51	12.52	19.71	12.88	5.27
190	23.45	3.17	45.79	15.11	3.84	3.74

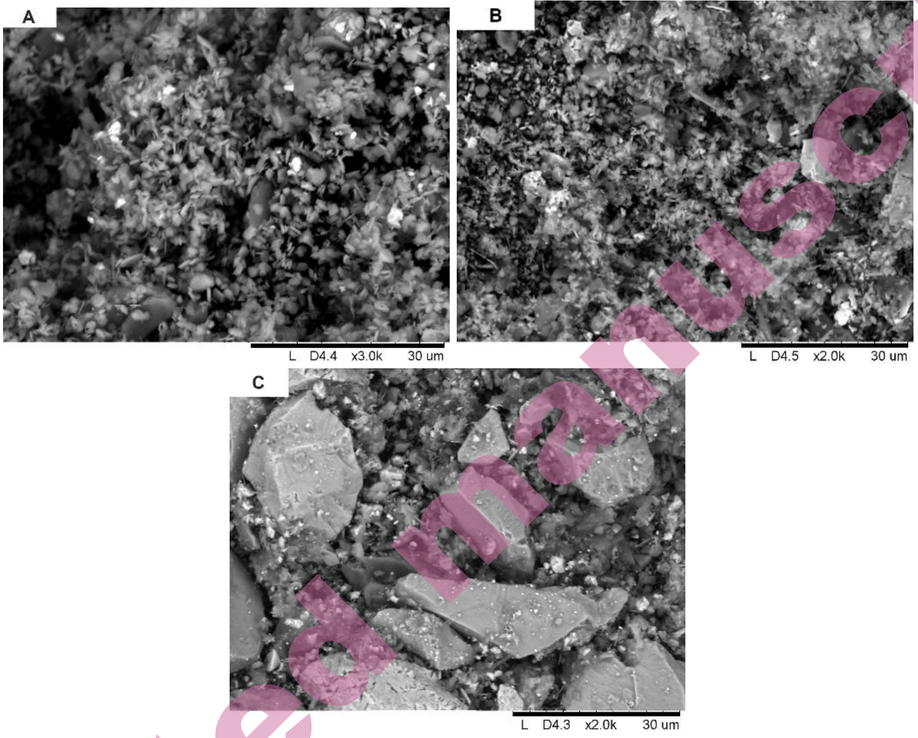

Fig 3. SEM image of solid residue after the leaching at 150 °C (A), 170 °C (B), and 190 °C(C)

According to the SEM/EDX analysis of the solid residue at 190 °C dissolution, elemental sulfur accounted for 3.17 % of the total sulfur. When the dissolution temperature was increased from 150 °C to 190 °C, the amount of undissolved chalcopyrite in the solid residue decreased from 10.75 % to 3.84 %, and the amount of elemental sulfur decreased and was transferred to the solution in the form of sulfate, increasing the amount of free sulfuric acid. However, the content of the pyrite was increased from 16.36 % to 45.79 %. The dissolution of pyrite minerals decreased with increasing temperature. The results showed that pyrite was more insoluble than chalcopyrite due to the relative hardness of chalcopyrite and pyrite 3.5-4 and 6-6.56, respectively. Moreover, during milling, the particle size of pyrite is bigger than that of chalcopyrite, which can be affected by reducing the specific surface area and reducing dissolution.[15]

Effect of sulfuric acid concentration and filtration condition

When the sulfuric acid concentration was increased from 30 g l^{-1} to 100 g l^{-1} at the leaching temperature of 150 °C and 190 °C, the leaching rate of copper and iron was compared in Figure 4 and Figure 5. As shown in Figure 4, the copper ion content varied from 40 g l^{-1} to 43.8 g l^{-1} when the solution was filtered with and without cooling, which was relatively close. However, the concentration of iron ions increased from 22 g l^{-1} to 27 g l^{-1} and 31.3 g l^{-1} to 34 g l^{-1} when the solution was filtered with and without cooling, respectively (at 150 °C).

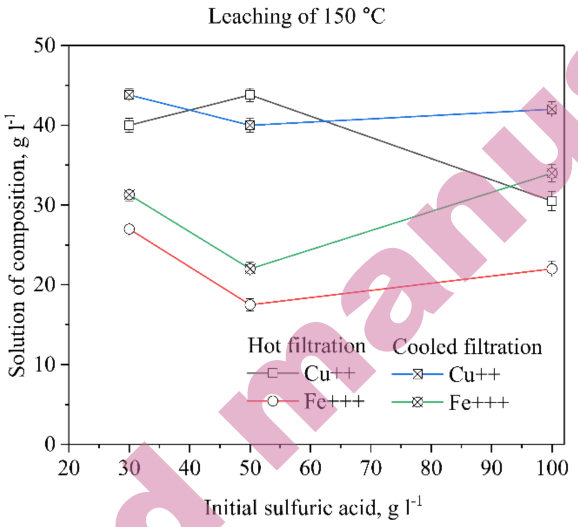

Fig 4. The effect of sulfuric acid concentration and filter condition on copper and iron dissolution at 150 ℃

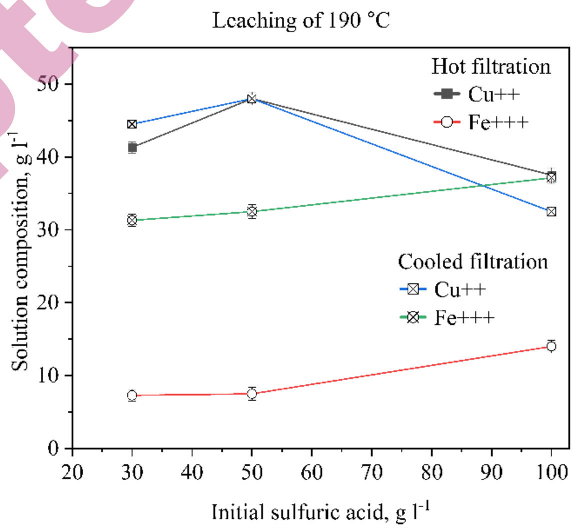

Fig 5. The effect of sulfuric acid concentration and filter condition on copper and iron dissolution at 190 ℃

Figure 5 illustrates the effects of increasing sulfuric acid concentration on metal dissolution at 190 °C. As the concentration of sulfuric acid rises from 30 g l^{-1} to 100 g l^{-1}, the leaching rate of copper slightly decreases while the leaching rate of iron increases. When the solution was rapidly filtered from the autoclave while still hot, the concentration of copper ions ranged from 41.3 g l^{-1} to 48 g l^{-1}, and the concentration of iron ions increased from 7.3 g l^{-1} to 14 g l^{-1}. Conversely, when the solution was filtered after cooling, the concentration of iron ions in the solution increased from 31.3 g l^{-1} to 37.14 g l^{-1}. Notably, at a sulfuric acid concentration of 50 g l^{-1}, copper dissolution peaked, resulting in an iron ion concentration of 7.5 g l^{-1}. These results indicate that rapidly separating the solution from the solid phase without allowing it to cool after pressure leaching is crucial for reducing ferric ions in the solution, as iron is precipitated as hematite during the oxidation pressure leaching process.

The X-ray diffraction patterns of the solid residue obtained from rapid filtration (without cooling) at temperatures of 150 °C and 190 °C are presented in Figure 6. The peaks corresponding to elemental sulfur and jarosite are generated at low temperatures (150 °C). At 190 °C, new peaks associated with the minerals jarosite and hematite were detected in the XRD pattern of the solid residue. The peaks of elemental sulfur disappeared at 190 °C, which indicates that the sulfur oxidized to sulfuric acid at high temperatures.

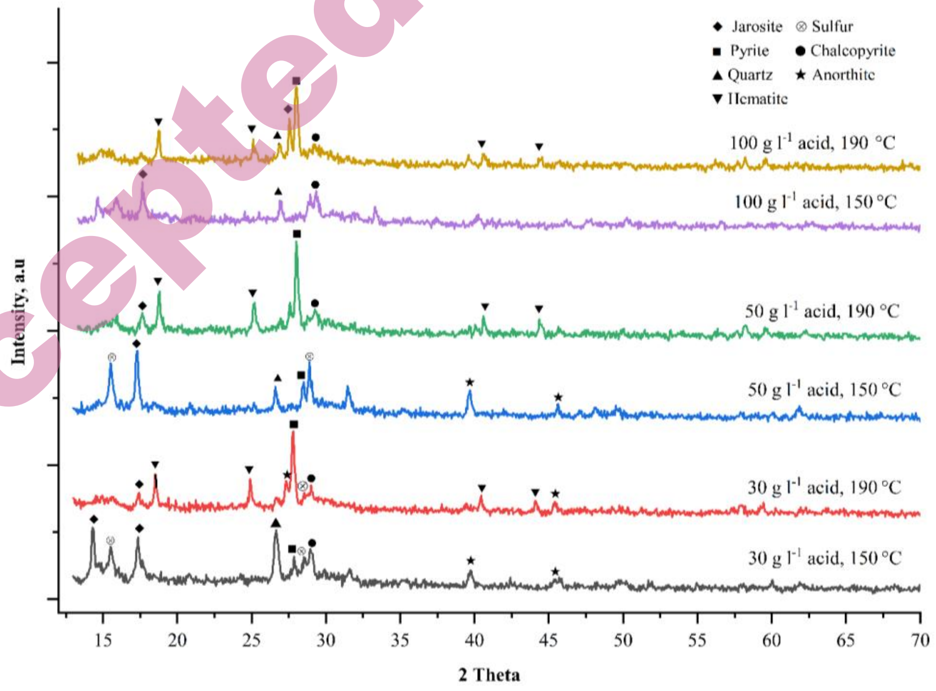

Fig 6. X-ray diffraction pattern of the solid residue formed rapid filtration (without cooling) of an autoclave solution

Figure 7 illustrates the X-ray diffraction patterns of the solid residue formed filtration after cooling. A general symptom was that a new peak for elemental sulfur was identified at 2θ = 27.78°, and the intensity of the peaks for the mineral pyrite generally decreased. This analysis suggests that elemental sulfur formed by the decomposition of chalcopyrite minerals transitioned from a solid to a liquid state between 150 °C and 190 °C, resulting in a reduced quantity of sulfur in the hot-filtered sample. Furthermore, during the cooling of the slurry, new elemental sulfur formed on the surface of the solid phase, as indicated by the X-ray diffraction results. The analysis results suggest that the amount of elemental sulfur detected in solid residue obtained from rapid filtration (without cooling) is expected to be low due to the elemental sulfur formed by the decomposition of chalcopyrite minerals must have transitioned from a solid to a liquid state at 150 °C and 190 °C. However, the X-ray diffraction pattern shows that new elemental sulfur is formed on the surface of the solid phase during the cooling of the slurry.

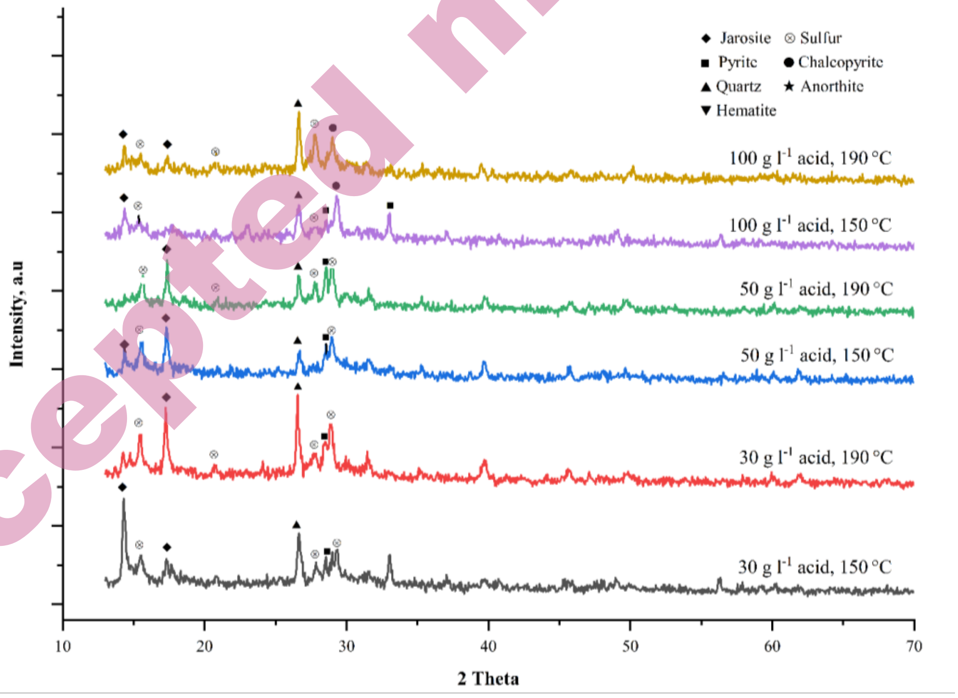

Fig 7. X-ray diffraction pattern of the solid residue formed filtration (with cooling) of an autoclave solution

Table 5 presents the analysis of free sulfuric acid content in leaching solution. It was observed that the amount of free sulfuric acid in the solution increased, while the peak for elemental sulfur was nearly absent in the solid residue at 190 °C (Figure 6 and Table 5). It suggests that the sulfide sulfur in the concentrate was converted to sulfate. Moreover, hematite in the solid residue (190 °C) indicates that iron sulfate, formed by the reaction, decomposed at this temperature to yield free sulfuric acid and hematite. As shown in Figure 7, the concentration of iron ions in the solution after rapid filtration decreased. This reduction can be expected to lead to the hydrolysis of iron ions in the solution, resulting in the formation of hematite in the solid residue.[7,16,17]

TABLE 5. Amount of free sulfuric acid in the leaching solution

H_2SO_4 initial concentration / g l^{-1}	Temperature / °C	Filtration condition	Free H_2SO_4 / g l^{-1}
30	150	Without cooling	28.59
		With cooling	22.12
30	190	Without cooling	64.63
		With cooling	40.49
50	150	Without cooling	46.78
		With cooling	42.72
50	190	Without cooling	88.11
		With cooling	46.99
100	150	Without cooling	62.15
		With cooling	62.04
100	190	Without cooling	117.6
		With cooling	92.925

Based on the above mentioned results, the iron content in the solution obtained from filtration with cooling increased from 7.5 g l^{-1} to 37.5 g l^{-1} (Figure 4), the intensity of the peak corresponding to the pyrite mineral decreased, and a new peak for hematite mineral was detected (Figure 7). It suggests that the following reaction may occur.[18–20]

Reactions in the system $CuSO_4 – H_2SO_4 – O_2 – H_2O$:

The main reaction that occurs at 150 °C

$$CuFeS_2 + 2Fe_2(SO_4)_3 = CuSO_4 + 5FeSO_4 + 2S^0 \quad (9)$$

$$2CuFeS_2 + 2.5O_2 + 5H_2SO_4 = 2CuSO_4 + Fe_2(SO_4)_3 + 4S^0 + 5H_2O \quad (10)$$

$$2FeSO_4 + H_2SO_4 + \frac{1}{2}O_2 = Fe_2(SO_4)_3 + H_2O \quad (11)$$

$$S^0 + O_2 + 2H_2O = 2H_2SO_4 \quad (12)$$

Jarosite formation reaction at 150 °C

$$Fe_2(SO_4)_3 + 3H_2O \rightarrow (H_3O)Fe_3(SO_4)_2(OH)_6 \quad (13)$$

The main reaction that occurs at 190 °C

$$CuFeS_2 + 16Fe_2(SO_4)_3 + H_2O = 2CuSO_4 + 34FeSO_4 + 16H_2SO_4 \quad (14)$$

$$2CuFeS_2 + 8.5O_2 + H_2SO_4 = 2CuSO_4 + Fe_2(SO_4)_3 + H_2O \quad (15)$$

$$2FeSO_4 + H_2SO_4 + ½\,O_2 = Fe_2(SO_4)_3 + H_2O \quad (16)$$

$$2S^0 + 3O_2 + 2H_2O = 2H_2SO_4 \quad (17)$$

Hematite formation reaction at 190 °C

$$2\mathrm{Fe_2(SO_4)_3} + 3\mathrm{H_2O} = \mathrm{Fe_2O_3} + 3\mathrm{H_2SO_4} \tag{18}$$

$$2\mathrm{Fe_2(SO_4)_3} + 3\mathrm{H_2O} \rightarrow 5\mathrm{H_2SO_4} + 3\mathrm{(H_3O)Fe_3(SO_4)_2(OH)_6} \tag{19}$$

CONCLUSION

1. When the dissolution temperature was increased from 150 °C to 190 °C, the amount of copper transferred to the solution increased from 89.27 % to 97.84 %, while the dissolution of iron decreased from 73.42 % to 65.42 %. However, the amount of elemental sulfur in the solid residue decreased from 39.09 % to 24.3 %, and the amount of iron increased.

2. When the sulfuric acid content was increased from 0.3 M to 1 M, the amount of copper transferred from the slurry to the solution increased from 40 g l^{-1} to 48 g l^{-1}. However, for iron, the content in the solution increased from 22 to 27 g l^{-1} and from 31.3 g l^{-1} to 34 g l^{-1} when the slurry was filtered without (rapidly) and with cooling.

3. Most of the sulfur in the initial concentrate remains as elemental sulfur in the solid residue, and the acid content in the solution decreases at low temperatures. However, at high temperatures, elemental sulfur is oxidized to sulfate, leading to an increase in the acid content of the solution.

4. Based on XRD analysis and experimental results, it can be concluded that as the dissolution temperature increases, the solubility of pyrite minerals decreases. As a result, iron ions in the solution undergo hydrolysis, forming new minerals such as jarosite and hematite. Therefore, the amount of iron transferred to the solution reduces while increasing the concentration of free sulfuric acid.

5. It was confirmed that the rapid separation of the solution from the solid phase without cooling after pressure leaching is crucial for decreasing ferric ions in the solution. If rapid filtration of the leach solution is not employed, the leaching solution will contain a significant amount of ferric ions. This high concentration of ferric ions creates issues in the subsequent neutralization step, as many copper ions will adsorb onto the iron hydroxide, making the slurry excessively thick. This thickness is a challenge in separating the solid and liquid phases during neutralization.

ИЗВОД

ОКСИДАТИВНО ЛУЖЕЊЕ БАКАРНОГ КОНЦЕНТРАТА ПОД ПРИТИСКОМ

GUNCHIN CHUNAG[1], ULZIIDELGER BYAMBASUREN[1], SARNAI ALTANTSETSEG[1], GANCHIMEG YUNDEN[1],
SUKHBAT SUKHBAATAR[2] И DORJGOTOV ALTANSUKH[1]

[1]*Department of Chemical Engineering, School of Applied Sciences, Mongolian University of Science and Technology, Ulaanbaatar 14191, Mongolia, and* [2]*Industrial Policy Department, Ministry of Industry and Mineral Resources, Ulaanbaatar, Mongolia.*

Ова студија је истраживала оксидативно лужење бакарног концентрата коришћењем смеше јона гвожђа(III) и раствора сумпорне киселине. Испитали смо утицаје различитих параметара, укључујући температуру, почетну концентрацију сумпорне киселине и услове филтрације суспензије. На нижим температурама (150 °C), процес лужења је резултирао формирањем елементарног сумпора и минерала јарозита у чврстом остатку. Насупрот томе, на вишим температурама (190 °C), чврсти остатак је садржао јарозит и хематит, при чему се већина елементарног сумпора оксидовала у сумпорну киселину. Под оптималним условима, температура лужења од 190 °C, однос концентрата и растварача за лужење (Fe^{3+} 5 g l^{-1} и H_2SO_4 50 g l^{-1}) од 1:8, притисак кисеоника од 1.0 MPaи величина честица чврсте фазе мања од 20 μm, стопа растварања бакра достигла је 98% након три сата. Када је концентрација сумпорне киселине повећана са 30 g l^{-1} на 100 g l^{-1}, количина бакра је повећана са 40 g l^{-1} на 48 g l^{-1}. Даље, брзо филтрирање раствора лужења без хлађења помогло је да се већина гвожђа задржи у чврстој фази, што је резултирало релативно чистим раствором. Чврсти остатак је анализиран помоћу рендгенске дифракције (XRD) и скенирајуће електронске микроскопије (SEM).

(Примљено 22. априла; ревидирано 17. маја; прихваћено 17. јуна 2024.)

REFERENCES

1. 2021/08, https://mrpam.gov.mn/public/pages/169/2021.08.stat.report.mon.pdf (accessed: april 2025)
2. N. Tumen-Ulzii, B. Gunchin, *J. Serbian Chem. Soc.* **88** (2023) 1149–1160 (https://doi.org/10.2298/JSC230114057T)
3. S. Wang, *Jom* **57** (2005) 48–51 (https://doi.org/10.1007/s11837-005-0252-5)
4. A. A. Baba, K. I. Ayinla, F. A. Adekola, M. K. Ghosh, O. S. Ayanda, R. B. Bale, A. R. Sheik, S. R. Pradhan, *Int. J. Min. Eng. Miner. Process.* **1** (2012) 1–16 (https://doi.org/10.5923/j.mining.20120101.01)
5. J. Cháidez, J. Parga, J. Valenzuela, R. Carrillo, I. Almaguer, *Metals (Basel).* **9** (2019) 189 (https://doi.org/10.3390/met9020189)
6. B. Han, B. Altansukh, K. Haga, Y. Takasaki, A. Shibayama, *J. Sustain. Metall.* **3** (2017) 528–542 (https://doi.org/10.1007/s40831-017-0135-3)
7. K. Takatori, H. Kato, A. Yoshimura, Y. Matsuno, *Mining, Metall. Explor.* **38** (2021) 1477–1485 (https://doi.org/10.1007/s42461-021-00400-3)
8. M. Sokić, B. Marković, S. Stanković, Ž. Kamberović, N. Štrbac, V. Manojlović, N. Petronijević, *Metals (Basel).* **9** (2019) 1173 (https://doi.org/10.3390/met9111173)
9. F. Saloojee, F. K. Crundwell, *J. South African Inst. Min. Metall.* **116** (2016) 517–524 (https://doi.org/10.17159/2411-9717/2016/v116n6a5)
10. S. Heguri, S. Asano, A. Idegami, *J. MMIJ* **131** (2015) 470–475 (https://doi.org/10.2473/journalofmmij.131.470)
11. S. Matuska, K. Ochromowicz, T. Chmielewski, *Physicochem. Probl. Miner. Process.* **54** (2018) 781–792 (https://bibliotekanauki.pl/articles/110420.pdf)
12. E. Uzun, M. Zengin, Ý. Atỳlgan, *Mater. Tehnol.* **50** (2016) 395–401 (https://doi.org/10.17222/mit.2015.091)
13. E. M. Córdoba, J. A. Muñoz, M. L. Blázquez, F. González, A. Ballester, *Hydrometallurgy* **93** (2008) 81–87 (https://doi.org/10.1016/j.hydromet.2008.04.015)
14. J. Gega, W. Walkowiak, *Physicochem. Probl. Miner. Process.* **46** (2011) 155 (https://www.dbc.wroc.pl/Content/10110/46_2011.pdf)

15. K. J. Nyembwe, E. Fosso-Kankeu, F. Waanders, M. Mkandawire, *Trans. Nonferrous Met. Soc. China (English Ed.* **31** (2021) 2139–2152 (https://doi.org/10.1016/S1003-6326(21)65644-3)
16. S. J. Petrović, G. D. Bogdanović, M. M. Antonijević, M. Vukčević, R. Kovačević, *Metals (Basel).* **13** (2023) 1818 (https://doi.org/10.3390/met13111818)
17. S. J. Petrović, G. D. Bogdanović, M. M. Antonijević, *Trans. Nonferrous Met. Soc. China (English Ed).* **28** (2018) 1444–1455 (https://doi.org/10.1016/S1003-6326(18)64788-0)
18. H. B. Zhao, M. H. Hu, Y. N. Li, S. Zhu, W. Q. Qin, G. Z. Qiu, J. Wang, *Trans. Nonferrous Met. Soc. China (English Ed.)* **25** (2015) 303–313 (https://doi.org/10.1016/S1003-6326(15)63605-6)
19. Y. Xing, C. Wei, Z. Deng, X. Li, M. Li, *Sci. Rep.* **14** (2024) 24490 (https://doi.org/10.1038/s41598-024-75857-5)
20. C. Li, Z. Deng, C. Wei, G. Fan, X. Li, M. Li, Y. Wang, *Hydrometallurgy* **178** (2018) 294–300 (https://doi.org/10.1016/j.hydromet.2018.05.012).